FINAL TECHNICAL REPORT
To: technicalreports@afosr.af.mil
Subject: FINAL TECHNICAL REPORT by Dr. Keiji Morokuma

Contract/Grant Title: Theoretical Studies of Gas Phase Elementary Reactions
Contract/Grant #: FA9550-07-1-00395
Reporting Period: 1 January 2007 to 30 November 2009

Accomplishment Summary:
The results of theoretical studies of gas phase elementary reactions are reported in the following topics. A. Development and Application of Liouville-von Neumann Dynamics Method for Efficient Direct Dynamics Calculations; B. Development of Global Reaction Route Mapping (GRRM) Method for Potential Energy Surface Exploration; C. R-Matrix Electron Scattering Calculations for Diatomic Molecules; D. Structure and Photochemistry of N_3Cl and N_3; E. Potential Energy Surfaces and Dynamics of Photodissociation of H_2CO; F. The Mechanism of Ion-Molecule Reaction: $POCl_3^-$ + O_2; G. Reactions of VX Agent.

Accomplishments:

A. Development and Application of Liouville-von Neumann Dynamics Method for Efficient Direct Dynamics Calculations

We developed a novel first principles Molecular Dynamics scheme, called LvNMD, based on the Liouville-von Neumann equation for density matrix propagation and the Magnus expansion of the time evolution operator. The scheme combines formally accurate quantum propagation of electrons represented via density matrix *P(t):*

$$i\hbar \frac{dP(t)}{dt} = [F(t), P(t)] \qquad (1)$$

and a classical propagation of R nuclear degrees of freedom:

$$\frac{dE}{dR} = M\frac{d^2R}{dt^2}, \qquad (2)$$

where *F = h + G(P)* is the Fock operator, M is mass of nuclei. E is the potential energy for nuclear motion obtained from electronic structure as a sum 1-electron, 2-electron and nuclear terms:

$$E = Tr[hP] + \frac{1}{2}Tr[G(P)P] + V_{NN} \qquad (3)$$

The solution to Eq. 1 is obtained via Baker-Campbell-Hausdorf (BCH) expansion.

$$P(t) = P(0) - it[F, P(0)] - \frac{t^2}{2!}[F,[F, P(0)]] + i\frac{t^3}{3!}[F,[F,[F, P(0)]]] + \ldots \qquad (4)$$

Some advantages of LvNMD are: (a) algorithm is free of constraint and fictitious parameters (different from ADMP (Atom-centered Density Matrix Propagation) and Car-Parrinello methods), (b) it avoids diagonalization of the Fock operator, and (c) it can be used in the case of fractional occupation. The last point is very important and it allows to effectively incorporate an ensemble of many states of nearly same energy (as found in transition metal clusters) via electronic temperature (Fermi-Dirac weighted density matrix). The algorithm has been found to be very stable and have a very good conservation of the total energy (see Figure 1 for comparison of energy conservation simulation of our LvNMD with BOMD (Born-Oppenheimer MD) and ADMP (Atom-centered Density Matrix Propagation) methods for a complex

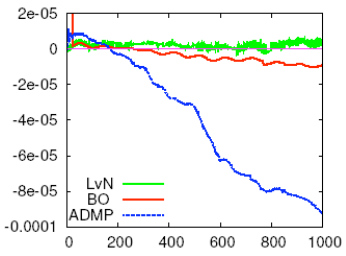

Figure 1. Conservation of energy for $Sc^+@C_{60}$ system for LvNMD, BOMD and ADMP methods as function of number of steps.

Report Documentation Page

Form Approved
OMB No. 0704-0188

1. REPORT DATE	2. REPORT TYPE	3. DATES COVERED
28 FEB 2010		**01-01-2007 to 30-11-2009**

4. TITLE AND SUBTITLE	5a. CONTRACT NUMBER
Theoretical Studies of Gas Phase Elementary Reactions	**FA9550-07-1-0395**
	5b. GRANT NUMBER
	5c. PROGRAM ELEMENT NUMBER
6. AUTHOR(S)	5d. PROJECT NUMBER
	5e. TASK NUMBER
	5f. WORK UNIT NUMBER
7. PERFORMING ORGANIZATION NAME(S) AND ADDRESS(ES)	8. PERFORMING ORGANIZATION REPORT NUMBER
Department of Chemistry,Emory University,1515 Dickey Dr.,Atlanta,GA,30322	
9. SPONSORING/MONITORING AGENCY NAME(S) AND ADDRESS(ES)	10. SPONSOR/MONITOR'S ACRONYM(S)
	11. SPONSOR/MONITOR'S REPORT NUMBER(S)

12. DISTRIBUTION/AVAILABILITY STATEMENT

Approved for public release; distribution unlimited

13. SUPPLEMENTARY NOTES

14. ABSTRACT

The results of theoretical studies of gas phase elementary reactions are reported in the following topics. A. Development and Application of Liouville-von Neumann Dynamics Method for Efficient Direct Dynamics Calculations; B. Development of Global Reaction Route Mapping (GRRM) Method for Potential Energy Surface Exploration; C. R-Matrix Electron Scattering Calculations for Diatomic Molecules; D. Structure and Photochemistry of N3Cl and N3; E. Potential Energy Surfaces and Dynamics of Photodissociation of H2CO; F. The Mechanism of Ion-Molecule Reaction: POCl3 - + O2; G. Reactions of VX Agent.

15. SUBJECT TERMS

16. SECURITY CLASSIFICATION OF:			17. LIMITATION OF ABSTRACT	18. NUMBER OF PAGES	19a. NAME OF RESPONSIBLE PERSON
a. REPORT	b. ABSTRACT	c. THIS PAGE			
unclassified	**unclassified**	**unclassified**	**Same as Report (SAR)**	**8**	

of endohedral fullerene and transition metal. A prototype code has been implemented with Gaussian suite for ab initio Hartree-Fock (HF) and density functional based tight-binding method (DFTB). Published as paper 10 in the archive below.

B. Development of Global Reaction Route Mapping (GRRM) Method for Potential Energy Surface Exploration. Efficient methods were developed for exploration of potential surfaces for large molecular systems as well as for finding the conical intersections and seams of crossing. Published as Paper 11 and 14.

C. R-Matrix Electron Scattering Calculations for Diatomic Molecules
We performed and published results of R-matrix calculations of differential cross sections for low-energy electron collisions with ground and electronically excited O_2 molecule as well as integral and differential cross sections for low-energy electron impact excitations of N_2 molecule. Dr. Tashiro, who wrote the code and performed calculations, became independent and is continuing work along the same line, and thus we stopped this project. Published as Paper 1 and 2.

D. Structure and Photochemistry of N_3Cl and N_3

Chemistry of choloroazide N_3Cl and hydrogen azide N_3H has attracted a substantial attention as a potential source of cyclic N_3 species, the simplest nitrogen high energy material, as well as in connection to the NCl-driven iodine chemical laser. Although we studied the N_3Cl. Previously we theoretically studied excited state dynamics of N_3H as well as the ground state potential surface and dynamics of N_3. In the present grant, we focused on the N-Cl bond energy and photodissociation dynamics of N_3Cl, as well as potential energy surfaces of excited states of N_3.

i. Dissociative photoionization of N_3Cl and the N-Cl bond energy in N_3Cl. This is a collaborative research with Alec Wodtke's high resolution synchrotron-radiation-based photoionization mass spectrometry experiment. Using the theoretically calculated binding energy of ClN_3^+ (0.2 eV), the *adiabatic* ionization potential of ClN_3 = 9.97± 0.02 eV was estimated. The measured appearance potentials for N_3^+, Cl^+, and N^+ provide three independent determinations of the Cl-N bond energy in ClN_3, leading to a new value of the N-Cl bond energy in ClN_3, $D_0(Cl\text{-}N_3)$=1.86 ± 0.05 eV, 0.3 eV lower than previously reported values. The high level *ab initio* (CCSD(T)) electronic structure calculations extrapolated to the complete basis set limit yield a value: $D_0(Cl\text{-}N_3)$=1.87 eV. This work has been published Paper 3.

ii. Possible pathway for formation of cyclic N_3 in 157nm photodissociation of N_3Cl. The photodissociation dynamics of chlorine azide (ClN_3) at the 157 nm region was studied theoretically using the multireference configuration interaction (MRCI) method and the complete active space (CASSCF) direct dynamics method. Based on the MRCI calculations, the excitation at the 157nm region was assigned to the $4^1A'(S_7) \leftarrow \tilde{X}\ ^1A'(S_0)$ transition. A likely pathway for the formation of cyclic N_3 after this transition was identified by direct CASSCF dynamics

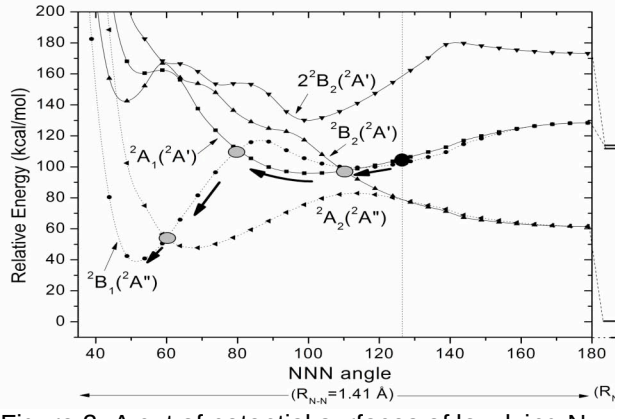

Figure 2. A cut of potential surfaces of low-lying N_3 doublet states in C_{2v} symmetry as a function of ∠NNN at a fixed R(N–N) of 1.41 Å. The large black dot indicates the beginning of the N_3 trajectory, and the large grey dots the conical intersections encountered. [sa(4)-CASSCF(15e/12o)/aug-cc-pVTZ level].

as follows (Figure 2). ClN_3 excited to $4^1A'(S_7)$ dissociates after about 40 fs to excited N_3 ($2^2A'$, with about 44 kcal/mol internal energy) + $Cl(^2P)$. This vibrationally hot $N_3(2^2A)$ goes diabatically through a conical intersection with $N_3(1^2A')$ at 44 fs onto $1^2A'$. At 19 fs later and repeatedly after every 55 fs, $N_3(1^2A')$ crosses and trickles down via Coriolis coupling to $N_3(2^2A''/^2B_1)$ state, which has a potential minimum at the cyclic-N_3 structure. Some fraction of $N_3(2^2A''/^2B_1)$ produced will survive dissociation and will be found as the cyclic-N_3, and some other fraction will eventually dissociate to $N(^2D) + N_2$ over a high barrier found previously. The paper has been published as Paper 4.

iii. Structures and energies of low-lying doublet excited states of N_3 from accurate configuration interaction calculations. The low-lying doublet excited states of the azide radical (N_3) have been studied at a highly-level multireference ab initio theory including basis sets up to augmented quadruple-ζ quality. A full hypersurface scan under C_{2v} restrictions for five low-lying bent N_3 states ($^2A_2$, $^2A_1$, $^2B_1$, and two $^2B_2$) revealed a highly complex potential surface manifold with many stationary points, conical intersections and multiple surface crossings, all of which have been characterized. The behavior of these states is discussed, especially as a function of the NNN angle. At least two new low-lying pathways on the excited surfaces leading from the linear to the cyclic-N_3 region were found, both involving the components of the degenerate excited $^2\Pi_u$ state of linear N_3. The paper was published as Paper 9.

v. Analytical potential energy surfaces for N_3 low-lying doublet states. Adiabatic potential energy surfaces (PESs) for five low lying doublet states (three $^2A'$ states and two $^2A''$ states) of N_3 are constructed based on 1504 single point calculations at the MRCISD(Q) level using aug-cc-pVTZ basis set. A new strategy is adopted to obtain the *final* PESs by combining *global* fits of individual adiabatic PESs and *local* simultaneous fits of two adiabatic PESs in several conical intersection regions with switching functions. See Figure 3, for example, for *local, global* and *final* PESs in the vicinity of conical intersection 1. These global fits employ basis functions that satisfy permutational invariance with respect to like nuclei, and have rms errors around 2-3 kcal/mol. The special local two-state fits are performed at the cyclic, bent and linear N_3 conical intersection regions to take account of intrinsic square root behavior of the potentials and thus to improve the quality of fitting. Stationary points as well as minima on the conical intersections and seams of crossing are located on these PESs and compared with *ab initio* results: the agreement is satisfactory in most cases. In addition to the construction of adiabatic PESs, diabatization is performed for the 1 $^2A'$ and 2 $^2A'$ states around their conical intersection at the N_3 bent region; these two diabatic PESs and diabatic coupling potential have been constructed and reported. This work has been published as Paper 8.

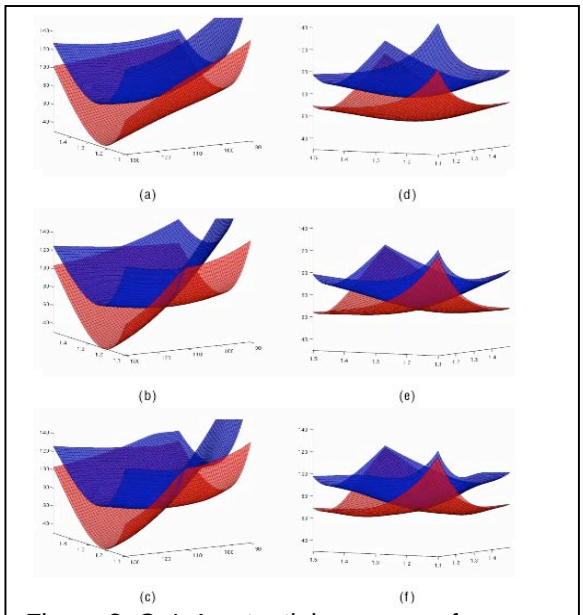

Figure 3. CoIn1 potential energy surfaces. (a),(d): surface from global fit; (b),(e): surface from local fit; (c),(f): final surface. r1 = r2 for (a), (b), (c); <NNN = 60º for (d), (e), (f).

E. Potential Energy Surfaces and Dynamics of Photodissociation of H_2CO

Formaldehyde has provided many opportunities to both experimentalists and theoreticians to study the mechanism of photodissociation as a simplest and prototypical molecule. However, the mechanism, in particular, how the molecule excited by radiation to the first singlet excited state (S_1) eventually comes down to the ground state (S_0) to dissociate mainly to H_2 + CO. A burst of theoretical activities has taken place in the last few years, and we have been one of the contributors to this exciting story.

i. Photodissociation dynamics of formaldehyde initiated at the T_1/S_0 minimum energy crossing configuration. The photodissociation dynamics of H_2CO is known to involve S_1, T_1 and S_0. Recent quasiclassical trajectory (QCT) calculations in conjunction with experiment have identified a "roaming" H-atom pathway to the molecular products, H_2+CO. These calculations were initiated at the global minimum (GM) of S_0, which is where the initial wavefunction is located. The "roaming" mechanism is not seen if trajectories are initiated from the molecular transition state saddle point (SP). In this work we identify the minimum energy-crossing configuration and energy of the T_1/S_0 potentials as a step towards studying the multi-surface nature of the photodissociation. QCT calculations are initiated at this configuration on a revised potential energy surface and the results are compared to those initiated, as previously, from the S_0 GM as well as the S_0 SP. This work has been published as Paper 5.

ii. Automated global mapping of minimal energy points on seams of crossing by the global reaction route mapping (GRRM) method: A case study on H_2CO. The automated global reaction route mapping (GRRM) method using the anharmonic downward distortion following (ADDF) procedure has previously been developed and applied to single potential energy surfaces (PESs). Dr. Satoshi Maeda who developed the method recently joined our group as Visiting Research Fellow. We have extended method to perform automated global mapping for minimal energy points on seams of crossing (MSX structures). Here the ADDF is applied to a penalty function based on two PESs of different electronic states. The present approach is effective not only for crossing seams between states with different symmetry but also for conical intersections for states with the same symmetry. As shown in Figure 4, many new MSX structures were discovered on the S_0/T_1 and S_1/T_1 crossing seams and the S_0/S_1 conical intersections of H_2CO by automated global mapping using the ADD-following method. A possible pathway for dissociation of formaldehyde excited to S_1 at low energy is discussed. This work was published as Paper 7.

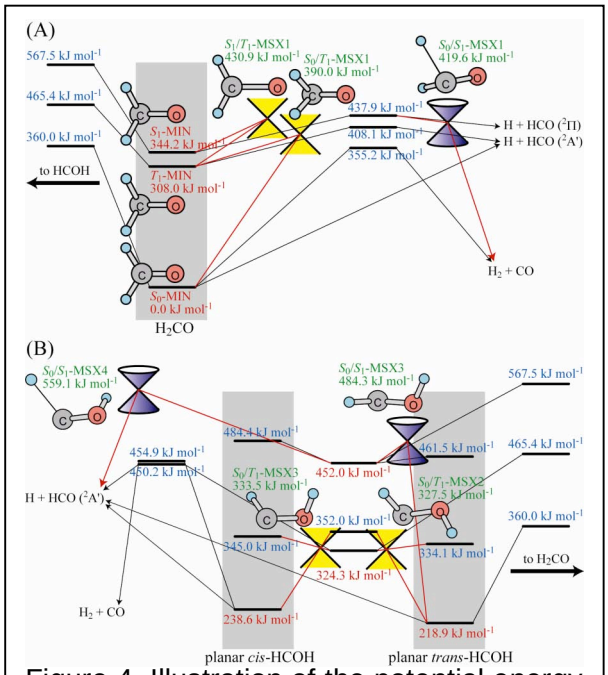

Figure 4. Illustration of the potential energy profiles for inside the potential wells of formaldehyde (A) and hydroxymethylene (B) based on the CASPT2 theory.

iii. Photochemical reactions of the low-lying excited states of formaldehyde. T_1/S_0 intersystem crossings, characteristics of the S_1 and T_1 potential energy surfaces, and a global T_1 potential energy surface. Accurate *ab initio* calculations using the multireference configuration interaction method have been performed to characterize the potential energy surfaces (PESs) of low-lying excited states (S_1 and T_1) of formaldehyde (H_2CO) and hydroxymethylene (HCOH) with emphasis on their isomerization, dissociation and the possible role of the T_1 state in the non-adiabatic photodissociation of H_2CO, as shown for T_1 in Figure 6.

Two regions on the T_1 PES are found to contribute to the non-adiabatic transition to the ground (S_0) state. Three minima on the seam of crossing (MSXs), 80~85 kcal/mol (above the S_0 global minimum), are located in the HCOH region; they however are blocked by a high-energy isomerization transition state at ~107 kcal/mol. The other MSX discovered in the H_2CO region is reachable with energy ≤ 91 kcal/mol and strong spin-orbit interaction; this may be a more important pathway for the T_1 to S_0 transition. A full-dimensional PES is generated for the T_1 state, fitted by a weighted least squares method employing a many-body expansion in which each term is a function of the internuclear distances and is invariant under permutations of like atoms. The single global function covers the formaldehyde and the hydroxymethylene regions as well as dissociation pathways. The high quality of the fitted PES is demonstrated by the small root-mean-square fitting error of 119 cm^{-1} and the close agreement between the critical points from *ab initio* calculations and from the fitted PES. This work was published as Paper 8.

F. The Mechanism of Ion-Molecule Reaction: $POCl_3^-$ + O_2

In the present experimental-theoretical joint efforts, the oxidation of the trichlorooxyphosphorus anion ($POCl_3^-$):

$$POCl_3^-(\tilde{X}\,^2A') + O_2(X\,^3\Sigma_g^-) \rightarrow PO_2Cl_2^-(\tilde{X}\,^1A') + ClO(X\,^2\Pi) + 45.4 \text{ kcal/mol}$$

which takes place in combustion flames has been examined experimentally in a variety of temperatures and theoretically via ab initio and density functional methods. The reaction was studied experimentally by the team of Dr. Al Viggiano using a turbulent ion flow tube (TIFT) and kinetics was measured between 300 and 626 K estimating an overall reaction barrier and reaction exothermicity of 1.23 and 45.4 kcal/mol, respectively. While a plethora of experimental data has been accumulated in the last few years about the reactivity of various oxyphosphorus compounds, there are virtually no detailed studies available that look into their reactivity from a theoretical standpoint. We have performed DFT and ab initio calculations of the potential energy surface involved in the reaction. As shown in Figure 2(A), we found at the UB3LYP/6-31+G* level that the reaction proceeds in the doublet state with a multi-step mechanism, in which reactants at first form a pre-reaction ion-molecule complex intermediate (Rcompl) and go over a barrier (TS0) to reach a five-coordinate trigonal bipyramidal (TBP) intermediate $[Cl_3P(O)(OO)]^-$ (LM0), which through a very skewed substitution (breaking a Cl-P bond and forming a Cl-O bond) transition state TS1 forms a chloroperoxy intermediate $[Cl_2P(O)(OOCl)]^-$ (LM1). Finally the OO bond is broken in LM1 via TS2 to form the product complex $[Cl_2P(O)O]^-(ClO)$ (Pcompl), which finally dissociates to the products $[Cl_2P(O)O]^-$ + ClO. Among various possible positions of ligands in the five-coordinate TBP complex, only two forms and thus two reaction pathways have been found to exist. The *equatorial* pathway involves attack of O_2 *cis* to the PO bond in $[Cl_3PO]^-$ giving the TBP intermediate $[Cl_3P(O)(OO)]^-$ (LM0) in which the O ligand is in the *equatorial* plane (see Fig. 2(A)), and the *axial* pathway has *trans* O_2 attack and the TBP intermediate with the O ligand (as well as the OO ligand) in the *axial* position (not shown). The rate-determining barrier is at TS1 and is about the same, 12.2 and 12.0 kcal/mol for equatorial and axial pathways, respectively, at the UB3LYP/6-31+G* level, and two pathways should compete against each other. DFT is knows to be unreliable in describe

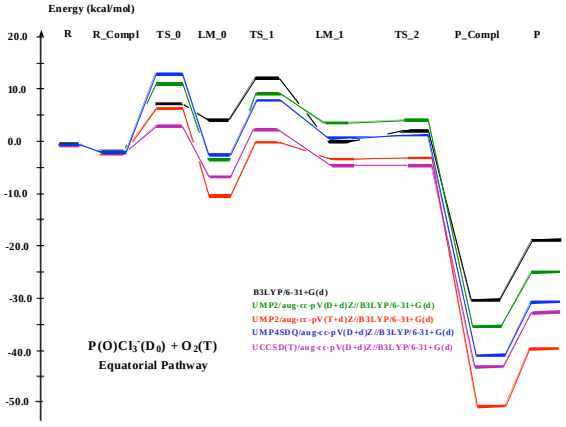

Figure 5. (A) Potential profile of the *equatorial* attack of O_2 to $POCl_3^-$ at the UB3LYP/6-31+G*

charge delocalization. Higher level single point calculations (shown in Figure 2(B)) lower the barriers substantially and give the barrier height for the *equatorial* pathway to be 3.2 and 2.5 kcal/mol at TS0 and TS1, respectively, at the UCCSD(T)//aV(D+d)Z level, in excellent agreement with the experiment. Radical-radical reactions usually have no or very small barrier. The (small) barrier in the present reaction seems to be caused by the energy required to deform the nearly tetrahedral reactant structure to a trigonal bipyramid structure at TS0 as well as small electron affinity of O_2 (0.45eV). The work was published as Paper 12.

G. Reactions of VX Agent

(i) Proton affinity and fluoride affinity of the VX toxic nerve agent. Protonation and fluorination were found to give various unique structures including dissociated species and ion molecule complexes.

(ii) Chemical ionization detection for monitoring of VX simulants with CIMS. An experimental and theoretical study was published as Paper 8.

Archival publications (published) during reporting period:

1. M. Tashiro, K. Morokuma and J. Tennyson, R-matrix calculation of differential cross sections for low-energy electron collisions with ground and electronically excited O_2 molecules, Phys. Rev. A 74, 022706/1-8 (2006).
2. M. Tashiro and K. Morokuma, R-matrix calculation of integral and differential cross sections for low-energy electron impact excitations of N_2 molecules, Phys. Rev. A, 75, 012720/1-10 (2007).
3. A. Quinto-Hernandez, Y.-Y. Lee, T.-P. Huang, W.-C. Pan, J. J.-M. Lin, P. Bobadova-Parvanova, K. Morokuma, P. C. Samartzis and A. M. Wodtke, Dissociative photoionization of ClN3 using high-resolution synchrotron radiation: The N-Cl bond energy in ClN_3, Int. J. Mol. Spec. 265, 261-266 (2007).
4. I. S. K. Kerkines, Z. Wang, P. Zhang, and K. Morokuma, Photodissociation of ClN_3 at 157 nm: Theory suggests a pathway leading to cyclic-N_3, J. Chem. Phys. 129, 171101/1-5 (2008).
5. B. C. Shepler, E. Epifanovsky, P. Zhang, J. M. Bowman, A. I. Krylov, and K. Morokuma, Photodissociation Dynamics of Formaldehyde Initiated at the T_1/S_0 Minimum Energy Crossing Configuration, J. Phys. Chem. A 112, 13267–13270 (2008).
6. Z. Wang, I. S. K. Kerkines, P. Zhang, and K. Morokuma, Analytical potential energy surfaces for N_3 low-lying doublet states, J. Chem. Phys. 130, 044313/1-18 (2009)
7. S. Maeda, K. Ohno, and K. Morokuma, Automated Global Mapping of Minimal Energy Points on Seams of Crossing by the Anharmonic Downward Distortion Following Method: A Case Study on H_2CO, J. Phys. Chem. A, 113, 1704-1710 (2009).
8. P. Zhang, S. Maeda, K. Morokuma and B. J. Braams, Photochemical reactions of the low-lying excited states of formaldehyde: T_1/S_0 intersystem crossings, characteristics of the S_1 and T_1 potential energy surfaces, and a global T_1 potential energy surface, J. Chem. Phys. 130, 114304/1-10 (2009).
9. I. S. K. Kerkines, Z. Wang, P. Zhang, and K. Morokuma, Structures and energies of low-lying doublet excited states of N_3 from accurate configuration interaction calculations, Mol. Phys. 107, 1017-1025 (2009).
10. J. Jakowski and K. Morokuma, Liouville-von Neumann Molecular Dynamics, J. Chem. Phys. 130, 224106/1-12 (2009)
11. S. Maeda, K. Ohno, and K. Morokuma, An Automated and Systematic Transition-Structure Explorer in Large Flexible Molecular Systems Based on Combined Global Reaction Route Mapping and Microiteration Methods, J. Chem. Theo. Comp. 5, 2734-2743 (2009).
12. I. S. K. Kerkines, K. Morokuma, N. Iordanova, and A. A. Viggiano, Experimental and Theoretical Study of the Reaction of $POCl_3^-$ with O_2, J. Chem. Phys. 132, 044309/1-9 (2010).

13. A. J. Midey, T. M. Miller, A. A. Viggiano, N. C. Bera, S. Maeda, and K. Morokuma, Chemical Ionization Detection for Monitoring of VX Simulants with CIMS, Anal. Chem. in press.
14. S. Maeda, K. Ohno, and K. Morokuma, Updated Branching Plane for Finding Conical Intersections without Derivative Coupling Vectors. J. Chem. Theo. Comp. in press.

Changes in research objectives, if any: None

Change in AFOSR program manager, if any: None

Extensions granted or milestones slipped, if any: None